ELSEVIER

MCN Molecular and Cellular Neuroscience

www.elsevier.com/locate/ymcne
Mol. Cell. Neurosci. 25 (2004) 83–94

# Altered expression of ion channel isoforms at the node of Ranvier in P0-deficient myelin mutants

Jochen C. Ulzheimer,[a] Elior Peles,[b] S. Rock Levinson,[c] and Rudolf Martini[a,*]

[a] *Section of Developmental Neurobiology, Department of Neurology, University of Wüerzburg, D-97080 Wüerzburg, Germany*
[b] *Department of Molecular Cell Biology, The Weizmann Institute of Science, Rehovot 76100, Israel*
[c] *Department of Physiology, University of Colorado Health Sciences Center, Denver, CO 80262, USA*

Received 25 July 2003; revised 17 September 2003; accepted 29 September 2003

**To elucidate the impact of myelinating Schwann cells on the molecular architecture of the node of Ranvier, we investigated the nodal expression of voltage-gated sodium channel (VGSC) isoforms and the localization of paranodal and juxtaparanodal membrane proteins in a severely affected Schwann cell mutant, the mouse deficient in myelin protein zero (P0). The abnormal myelin formation and compaction was associated with immature nodal cluster types of VGSC. Most strikingly, P0-deficient motor nerves displayed an ectopic nodal expression of the $Na_v1.8$ isoform, where it is coexpressed with the ubiquitous $Na_v1.6$ channel. Furthermore, Caspr was distributed asymmetrically or was even absent in the mutant nerve fibers. The potassium channel $K_v1.2$ and Caspr2 were not confined to juxtaparanodes, but often protruding into the paranodes. Thus, deficiency of P0 leads to dysregulation of nodal VGSC isoforms and to altered localization of paranodal and juxtaparanodal components of the nodal complex.**


## Introduction

The node of Ranvier of myelinated axons is the critical functional region for the generation and saltatory propagation of action potentials in the central (CNS) and peripheral nervous system (PNS). The subcellular and molecular architecture of the node and of its neighboring domains, namely, the paranodal and juxtaparanodal compartments, is highly differentiated (Arroyo and Scherer, 2000; Peles and Salzer, 2000; Scherer and Arroyo, 2002). This is reflected by the finding that the formation of the paranodal region is dependent on trans-interacting cell surface components such as contactin and contactin-associated protein (Caspr, also called paranodin) on the axolemma and neurofascin 155 on the paranodal glial membrane (Charles et al., 2002). The juxtaparanodal compartment is characterized by the expression of Caspr2 and by the concentration of axon-related voltage-gated $K^+$ channels (Coetzee et al., 1999; Poliak et al., 1999; Rasband et al., 1999) and TAG-1 (Traka et al., 2002).

Of particular interest is the clustering of voltage-gated sodium channels (VGSCs) at the nodal axolemma. In comparison to the internodes, the nodal VGSCs are highly concentrated and most probably linked to the underlying cytoskeleton by ankyrinG via their associated β-subunits (Bennett and Lambert, 1999; Jenkins and Bennett, 2001, 2002; Kordeli et al., 1995; Malhotra et al. 2000). In the PNS, this nodal clustering of sodium channels is dependent on direct contact with Schwann cells (Vabnick et al., 1996) which induce an accumulation of ankyrinG (Lambert et al., 1997), and the typical clustering of the VGSCs (Ching et al., 1999; for review, see Girault and Peles, 2002).

VGSCs consist of a pore-forming α-subunit (approximately 250 kDa) and one or two β-subunits (for review, see Isom, 2001). In the nervous system, one of the most highly abundant isoforms of the α-subunit is $Na_v1.6$ (formerly named PN4 or Nach6, corresponding to the SCN8A gene; Goldin, 1999; Krzemien et al., 2000; for review, see Novakovic et al., 2001), which is sensitive to tetrodotoxin (TTX) and is fast inactivating. $Na_v1.2$ is transiently expressed during myelination at forming nodes of Ranvier in rat peripheral nerve fibers, where it is rapidly replaced by $Na_v1.6$ with maturation of the nodes (Boiko et al. 2001). In contrast to these isoforms, $Na_v1.5$, $Na_v1.8$ and $Na_v1.9$ channels are TTX-resistant and are slowly inactivating. $Na_v1.8$ (formerly called SNS or PN3, corresponding to the SCN10A gene located on human chromosome 3p21-24; Akopian et al., 1996; Kozak and Sangameswaran, 1996, Novakovic et al., 2001; Sangameswaran et al., 1996) is exclusively present at the nodes of Ranvier of a restricted subpopulation of small-diameter dorsal root ganglia and trigeminal neurons where they may play a role in nociception (Novakovic et al., 1998). In motor nerves, this isoform is not detectable under normal conditions. Thus, distinct isoforms of VGSC are differentially distributed in myelinated nerve fibers in different nerve types.

Since in the PNS the clustering of nodal VGSCs is strictly dependent on myelinating Schwann cells (see above), we were interested in the organization and isoform expression of channels when myelination is abnormal. For this purpose, we investigated mice homozygously deficient in the myelin protein P0 (also called myelin protein zero, MPZ). These mutants show a severe and early

* Corresponding author. Section of Developmental Neurobiology, Department of Neurology, University of Wuerzburg, Josef-Schneider-Strasse 11, D-97080 Wuerzburg, Germany. Fax: +49-931-20123697.
*E-mail address:* rudolf.martini@mail.uni-wuerzburg.de (R. Martini).
**Available online on ScienceDirect (www.sciencedirect.com.)**

1044-7431/$ - see front matter © 2003 Elsevier Inc. All rights reserved.
doi:10.1016/j.mcn.2003.09.015

onset dysmyelinating neuropathy characterized by myelin decompaction, myelin degeneration and axonopathic changes (Frei et al., 1999; Giese et al., 1992; Martini et al., 1995a). As well, the formation of paranodal E-cadherin-mediated adherens junctions in Schwann cells had been shown to be altered in these mice (Menichella et al., 2001). Here, we found an abnormal clustering of VGSCs in this dysmyelinating mutant: Many fibers displayed cluster patterns typical for developing rather than mature fibers. Moreover, the $Na_v1.8$ channel isoform was abundantly expressed in nodes of motor nerves that are devoid of this channel type in wild-type (WT) mice. Additionally, in the paranodal region, Caspr was often expressed asymmetrically and potassium channels and Caspr2 were often shifted from the juxtaparanodal compartment to the paranode or were even not detectable. These findings demonstrate that normal myelination is not only an important prerequisite for the molecular organization of the nodal environs but also for

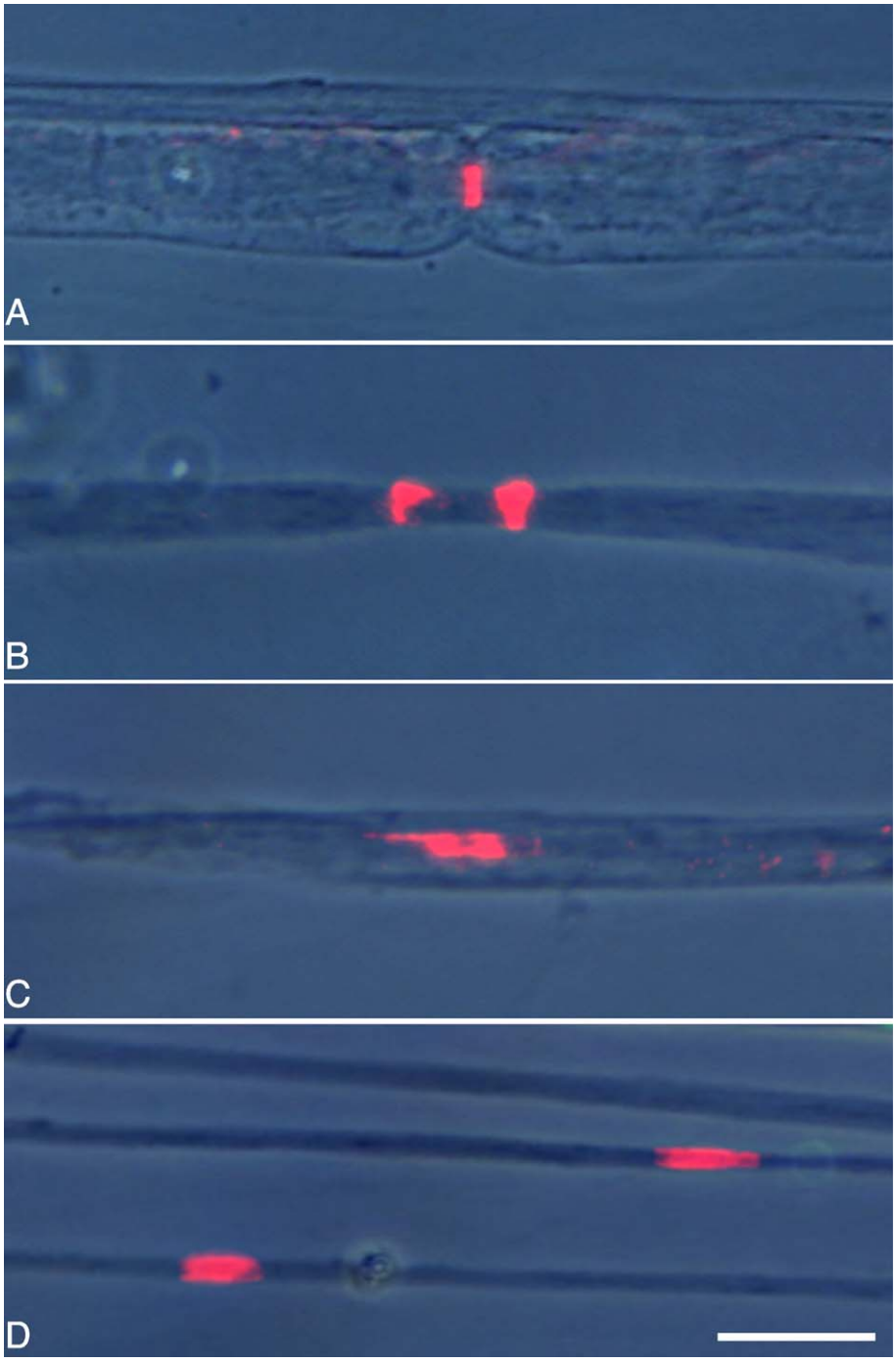


Fig. 1. Peripheral nerves of WT mice display mature VGSC clusters at the nodes of Ranvier. Their diameter/length ratio typically ranges from approximately 2 to 3 (A). P0 −/− nerves display nodal VGSC cluster types resembling developmentally immature intermediates such as paired clusters (B), binary clusters (C) and broad clusters (D). Teased fiber preparation of sciatic nerve (C and D) or quadriceps nerve (A and B) of 3 month-old WT (A) and P0 −/− mice (B–D), stained with rabbit pan-specific anti-$Na_v$-antibody (red). Overlay of fluorescence and phase contrast images. Scale bar, 10 μm.

the expression of the appropriate VGSC isoforms in distinct fiber types.

## Results

### *Sodium channel clusters of adult P0−/− mice are reminiscent of immature clusters in myelinating nerves of WT mice*

At the mature nodes of Ranvier of 3 month old WT mice, axon diameters are typically reduced in a funnel-shaped manner between the adjacent paranodes of the neighboring myelinating Schwann cells. Here, VGSC clusters form a slim ring of approximately 1 μm length. Typically, mature VGSC clusters appear as rectangular profiles with a diameter/length ratio of approximately 2 to 3 in large caliber fibers and approximately 1 or less in small caliber fibers. In nerve fibers of P0−/− animals, nodes display predominantly broader appearing VGSC clusters with a typical diameter/width ratio less than 1, mostly in the range of 0.2 to 0.6, (data not shown). This is especially prominent in small caliber fibers. This cluster shape resembles developmental stages of VGSC clusters as they occur during myelination (Vabnick et al., 1996; for review, see Rasband and Trimmer, 2001). In addition, a significant proportion of nodal profiles show binary or broad clusters, which are not detectable in WT nerves even at a younger age of 2 months (Fig. 1). Besides these, there are VGSC clusters resembling mature clusters of WT mice (Table 1). Typically, the nodal profiles of binary, broad and mature clusters can be simultaneously found in the same fiber preparation.

### *Internodal length is reduced in P0−/− nerve fibers*

To quantify internodal length, teased fibers of sciatic, quadriceps and saphenous nerves were double-stained for Caspr and $Na_v1.6$. Nodal profiles were identified by either the presence of typical nodal VGSC clusters or paranodal Caspr. The number of nodal profiles was determined in relation to the cumulative fiber length inversely reflecting internodal length. In WT femoral quadriceps nerve, 1.0 ± 0.1 nodal profiles per millimeter were counted, whereas this value was 2.0 ± 0.3 nodes per millimeter in saphenous nerve, reflecting a half as long internodal length in the sensory cutaneous nerve (1000 and 500 μm, respectively). By contrast, in P0−/− quadriceps and saphenous nerve, 3.4 ± 0.2 and 4.0 ± 0.6 nodes per millimeter, respectively, were counted corresponding to a respective internodal length of 250 and 294 μm (for absolute numbers and fiber length counted, compare Table 2).

Table 1
Teased fiber preparations of P0 − / − femoral quadriceps nerve (“Quadriceps”), saphenous nerve (“Saphenous”) and sciatic nerve (“Sciatic”) were stained with a pan-specific VGSC antibody

| Nerve | Mature (%) | Intermediate (%) | Broad (%) | Binary/ paired (%) |
|---|---|---|---|---|
| Quadriceps | 31.4 | 56.5 | 5.8 | 6.3 |
| Saphenous | 25.8 | 63.4 | 3.8 | 7.0 |
| Sciatic | 12.6 | 79.4 | 5.4 | 2.6 |

VGSC clusters have been counted and categorized for mature (diameter/length ratio approximately 2 to 3), broad (diameter/length ratio approximately < 0.6), intermediate (diameter/length ratio between 0.6 and 2) or binary/paired appearance. In WT nerves, only mature clusters were seen (data not shown). Given are the percentages of each category’s nodal profiles of the respective totals of counted VGSC-positive profiles, which figure 207, 186 and 1142 profiles in quadriceps, saphenous and sciatic nerve, respectively.

Table 2
In teased fiber preparations of WT and P0 − / − femoral quadriceps nerve (“Quadriceps”), saphenous nerve (“Saphenous”) and sciatic nerve (“Sciatic”) nodal profiles were identified by paranodal Caspr and/or typical nodal staining for $Na_v1.6$ and analyzed for presence or absence of nodal $Na_v1.6$ clusters

| WT | $Na_v1.6$ positive (*n*) | $Na_v1.6$ negative (*n*) | Fiber length counted (mm) |
|---|---|---|---|
| Quadriceps | 150 | 7 | 158 |
| Saphenous | 181 | 44 | 106 |
| Sciatic | 168 | 61 | 237 |
| **P0−/−** | **$Na_v1.6$ positive (*n*)** | **$Na_v1.6$ negative (*n*)** | **Fiber length counted (mm)** |
| Quadriceps | 521 | 63 | 156 |
| Saphenous | 579 | 82 | 154 |
| Sciatic | 383 | 66 | 160 |

The absolute numbers of nodal profiles counted and the cumulative fiber length examined are indicated. P0−/− as well as WT nerves showed predominant positivity for $Na_v1.6$. However, in the motor quadriceps nerve, tendentially more nodes are negative for $Na_v1.6$ in P0−/− mice (for percentages and *t* test, see text).

### *The TTX-sensitive $Na_v1.6$ isoform is preserved and the TTX-resistant $Na_v1.8$ isoform is upregulated at nodes of Ranvier of P0−/− mice*

The TTX-sensitive $Na_v1.6$ channel is the predominant VGSC isoform at adult nodes of Ranvier (Caldwell et al., 2000; Tzoumaka et al., 2000). Accordingly, we found that in femoral quadriceps nerves of WT mice, almost all nodal profiles (95.8 ± 1.9%), and in saphenous and sciatic nerve, the vast majority of nodes (79.8 ± 1.5% and 84.2 ± 2.9%) are positive for $Na_v1.6$ (Figs. 2A and 3A). In P0−/− mice, these percentages are not significantly different (87.2 ± 4.6%, 84.2 ± 3.0% and 82.0 ± 2.0%, respectively, Fig. 2A; for absolute numbers, see Table 2). $Na_v1.6$-positive nodes of WT fibers solely display mature clustering (Fig. 3A), whereas broad and binary clusters are frequent in P0−/− mice (Fig. 3B). Due to the identification of nodal profiles by VGSC-independent Caspr staining, nodes negative for $Na_v1.6$ could be unequivocally detected as well. As a trend, in P0−/− femoral quadriceps nerves, more nodal profiles negative for $Na_v1.6$ were detected than in WT (12.8 ± 4.6% vs. 4.2 ± 1.9%, $P = 0.35$; see Fig. 2A).

In WT peripheral nerves, TTX-resistant $Na_v1.8$ isoforms are normally restricted to a subpopulation of sensory fibers (Akopian et al., 1996; Novakovic et al., 1998), putatively nociceptive fibers (Baker and Wood, 2001). Accordingly, in teased fiber preparations of WT nerves, some subpopulations of fibers show $Na_v1.8$-positive nodal profiles in saphenous sensory and the mixed sciatic nerves. Since isotype-specific antibodies against VGSC were only available from one species (rabbit), we could not reliably show by a direct double immunofluorescence whether there is a coexpression of both isoforms in some fibers. However, since the sums of the percentages of $Na_v1.6$- and $Na_v1.8$-positive nodes in sciatic and

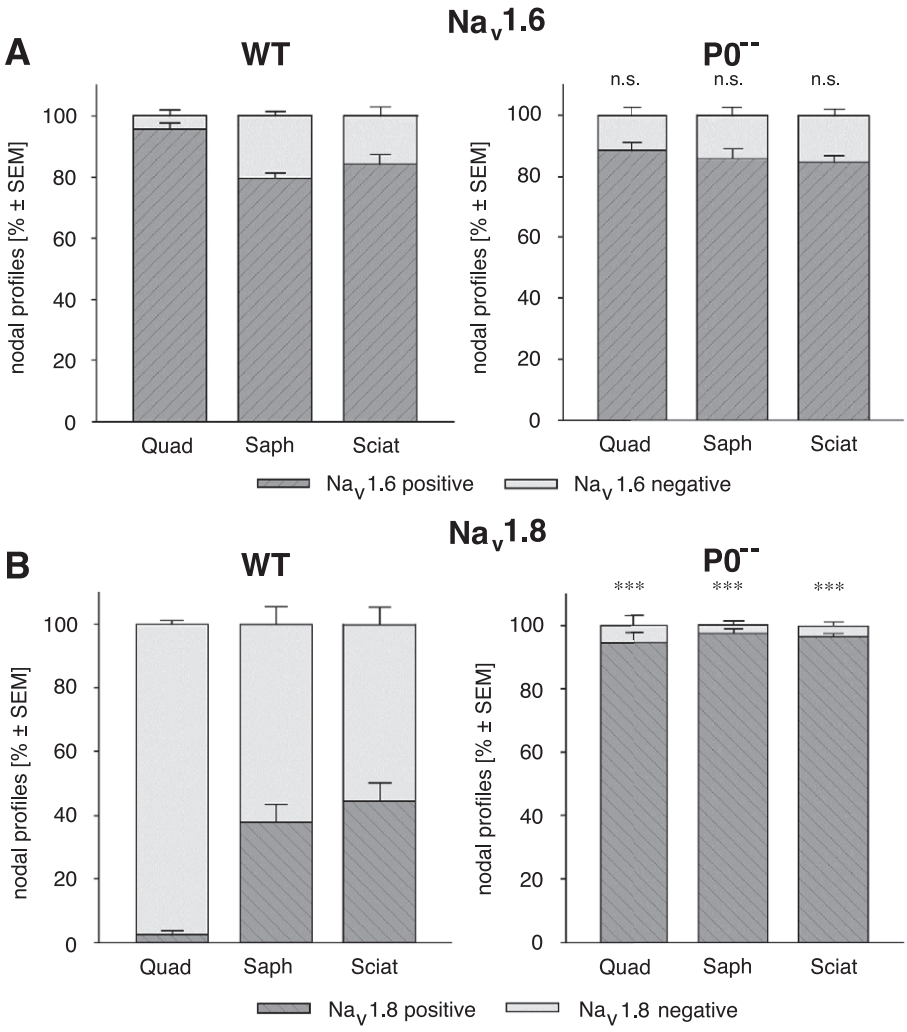


Fig. 2. $Na_v1.6$ is preserved and $Na_v1.8$ is upregulated at the nodes of P0−/− nerve fibers of motor (femoral nerve, quadriceps branch, "Quad"), sensory (saphenous nerve, "Saph") and mixed nerves (sciatic nerve, "Sciat"). Nodal profiles of teased fiber preparations were identified by either typical VGSC clusters or adjacent Caspr expression and analyzed for positivity (dark hatched column segments) or negativity (clear column segments) for $Na_v1.6$ (A) or $Na_v1.8$ (B), respectively. Results are taken from immunofluorescence-stained teased nerve fibers using polyclonal rabbit anti-$Na_v1.6$ or anti-$Na_v1.8$ antibodies in parallel to mouse anti-Caspr antibody. Differences in the number of VGSC-isoform-positive nodes between WT and P0−/− genotypes were submitted to *t* test for each nerve type separately.

saphenous nerves exceed 100 (Figs. 2A and B, left sides), it must be concluded that some nodes carry both isoforms.

In contrast to saphenous and sciatic nerve, the $Na_v1.8$ isoform is almost absent from the WT femoral quadriceps motor nerve (Figs. 2B and 3C; for absolute values, see Table 3).

When investigating nodes of Ranvier in P0−/− mice, a strong increase in $Na_v1.8$-positive nodes was detectable (Figs. 2B, 3D, 3F and 3G). Particularly striking is the upregulation in femoral quadriceps nerve where almost all nodes expressed the TTX-resistant isoform, whereas in the same nerve of WT mice, the $Na_v1.8$ isoform was barely detectable. By their comparison, the percentages of $Na_v1.6$- and $Na_v1.8$-positive nodes in all nerves (Figs. 2A and B, right sides) suggest that most nodes express both isoforms in P0−/− mice.

We also investigated the expression of the TTX-sensitive $Na_v1.2$ isoform in sciatic and quadriceps nerve fiber preparations of WT and P0−/− mutants. Neither of the genotypes displayed $Na_v1.2$ immunoreactivity in peripheral nerve fibers (not shown). However, nodal staining was obtained in fresh-frozen sections of optic nerves from newborn and 3-month-old WT mice (not shown), proving the reactivity of the $Na_v1.2$ antibodies used.

### *Altered paranodal localization of Caspr in P0−/− nerve fibers*

WT nodes of Ranvier are symmetrically bordered by Caspr, which is localized to the paranodes and adjacent to the inner mesaxon along the internode of either side of the node (Figs. 3A, C and E). By contrast, in P0−/− nerve fibers, Caspr staining was found to be more often asymmetrical with respect to the paranodal and internodal localization or even absent from either side of the node. In WT quadriceps nerve, 96.9 ± 0.5% of nodal profiles show symmetrical Caspr staining, in P0−/− quadriceps nerve, this number is reduced to 41.9 ± 3.9 (Figs. 4 and 5A). Instead, 53.1 ± 3.6% are asymmetrical and 5.0 ± 1.2% are completely negative for Caspr (Figs. 4 and 5B). This asymmetry does not only refer to

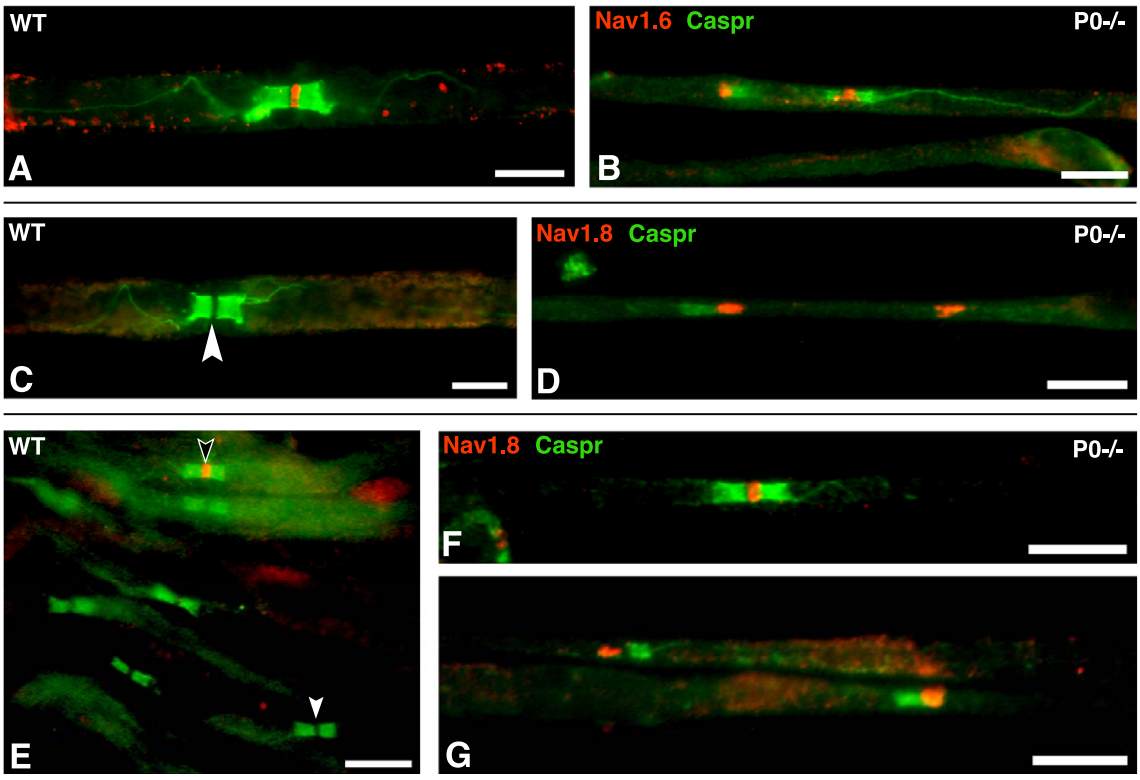


Fig. 3. $Na_v1.6$ is the predominant VGSC at the node of Ranvier in WT nerve fibers (A, red). There it is symmetrically flanked by paranodal Caspr (green). In P0−/− fibers, $Na_v1.6$ is still present at the node, but often abnormally clustered resembling immature cluster intermediates and asymmetrically flanked by Caspr (B). At nodes of WT motor nerves, $Na_v1.8$ is not expressed (C, arrowhead), whereas it is present in almost all P0−/− nodes (D, red). These often display paranodal asymmetry for Caspr (D, green). By contrast, in WT sensory nerves, $Na_v1.8$ is expressed in a small subpopulation of nodes, presumably belonging to nociceptive fibers (E, red, black arrowhead), others are devoid of $Na_v1.8$ (white arrowhead). At nodes of P0−/− sensory fibers, $Na_v1.8$ is generally increased (F, red). Note the paranodal asymmetry of Caspr (G, green). Teased fiber preparations of femoral quadriceps nerve (A–D) and saphenous nerve (E–G) immunostained for $Na_v1.6$ (red, A and B), $Na_v1.8$ (red, C–G) and Caspr (green, A–G). Scale bars, 10 μm.

the paranodal expression but also to the internodal expression of Caspr along the inner mesaxon, which is only present at one side of the node in asymmetrical profiles (Fig. 5B). Strikingly, nodal profiles in P0−/− quadriceps nerve devoid of $Na_v1.8$, which are representing morphologically normal nodes of Ranvier, display exclusively symmetrical Caspr staining.

*Expression of $K^+$ channels and Caspr2 is altered in the nodal region of P0−/− nerve fibers*

The paranodal junction which is demarcated by Caspr spatially separates nodal VGSC from juxtaparanodal $K^+$ channels. Mutations in paranodal molecules (e.g. Caspr and contactin deficiency) lead to an altered localization of potassium channels (Bhat et al., 2001; Boyle et al., 2001). Since we found an abnormal localization of paranodal Caspr in P0−/− nerves, we investigated the distribution of $K_v1.2$ subunits. In agreement with previous reports (Rasband et al., 1999), we found that almost all juxtaparanodal regions are $K_v1.2$ positive in WT quadriceps and sciatic nerves and this expression is always symmetrical with regard of the node (Figs. 6 and 7). There was no paranodal localization or absence of $K_v1.2$ to be found in WT mice. In quadriceps nerves of P0−/− mice, however, symmetrically labeled juxtaparanodes were rarely seen. Instead, we found the majority of nodal regions with abnormal $K_v1.2$ localization, particularly displaying a shift of $K_v1.2$ to the paranodes or at least an expansion of juxtaparanodal $K_v1.2$ to the paranodes (in 43.0 ± 2.6% of all nodal profiles). In addition, juxtaparanodal and paranodal $K^+$ channels are often asymmetrically distributed and 29.5 ± 5.2% of the nodal profiles do not express $K_v1.2$ at its environs at all (Figs. 6 and 7).

Similarly, expression of Caspr2, which normally is confined to the juxtaparanodes in WT nerves, is altered in P0−/− mice. In these mutants, Caspr2 is often shifted or expanded to the paranode in the majority of nodal profiles (72.9 ± 4.8%) where it is partially overlapping with Caspr (Figs. 7 and 8). Only 5.3 ± 1.5% are symmetrically localized to the juxtaparanodes, whereas a considerable percentage of nodal profiles is entirely devoid of Caspr2 (6.7 ± 2.6%).

## Discussion

In the present study, we could show that deficiency in the myelin protein P0, a transmembrane adhesion molecule involved in the formation and maintenance of compact myelin, affects the clustering of VGSCs at the node of Ranvier in two ways. First, nodal VGSC clusters reminiscent of developmentally retarded stages were abundantly present. Second, P0−/− deficient motor nerves displayed an ectopic expression of the TTX-resistant $Na_v1.8$ isoform at the nodes, where it is obviously coexpressed with the nearly ubiquitous $Na_v1.6$

Table 3
In teased fiber preparations of WT and P0 −/− femoral quadriceps nerve ("Quadriceps"), saphenous nerve ("Saphenous") and sciatic nerve ("Sciatic") nodal profiles were identified by paranodal Caspr and/or typical nodal staining for $Na_v1.8$ and analyzed for presence or absence of nodal $Na_v1.8$ clusters

| WT | $Na_v1.8$ positive (*n*) | $Na_v1.8$ negative (*n*) | Fiber length counted (mm) |
|---|---|---|---|
| Quadriceps | 4 | 266 | 220 |
| Saphenous | 109 | 192 | 127 |
| Sciatic | 105 | 123 | 189 |
| **P0−/−** | **$Na_v1.8$ positive (*n*)** | **$Na_v1.8$ negative (*n*)** | **Fiber length counted (mm)** |
| Quadriceps | 424 | 73 | 321 |
| Saphenous | 547 | 18 | 130 |
| Sciatic | 713 | 35 | 214 |

The absolute numbers of nodal profiles counted and the cumulative fiber length examined are indicated. WT motor nerves (quadriceps) display almost no $Na_v1.8$-positive nodes, whereas sensory (saphenous) and mixed nerves (sciatic) show a considerable percentage of $Na_v1.8$-positive nodes. By contrast, all P0−/− nerves show a strong upregulation of $Na_v1.8$. The number of $Na_v1.8$ negative nodes is dramatically reduced (for percentages and *t* test, see text).

isoform. In addition to these alterations at the node proper, asymmetry or even absence of the paranodal Caspr, and abnormal localization of juxtaparanodal $K^+$ channels and Caspr2 could be detected in these mutants. Thus, the finding that P0 deficiency leads to dysregulation of nodal $Na_v$ isoforms and to an altered localization of paranodal and juxtaparanodal molecules supports the idea that intact myelinating Schwann cells are necessary to determine the isoform expression of VGSCs at the node of Ranvier and to direct $K^+$ channels and Caspr2 to their juxtaparanodal sites.

A similar dislocation of the usually juxtaparanodal $K^+$ channels and Caspr2 has also been observed in knock-out mutants lacking the paranodal proteins Caspr and contactin (Bhat et al., 2001; Boyle et al., 2001; Poliak et al., 2001). Similarly, mice lacking galactocerebroside and sulfatide (Dupree et al., 1999; Ishibashi et al., 2002; Poliak et al., 2001), the PLP-mutants *md* rats (Arroyo et al., 2002) and *jimpy* mice (Jenkins and Bennett, 2002) are devoid of Caspr and display comparable alterations in paranodes and juxtaparanodes. Typically, in all these mutants, the dislocation of the juxtaparanodal molecules shows a rather uniform pattern in that $K^+$ channels and Caspr2 are found shifted to the paranodes where they appear to abut or even overlap with the nodal VGSCs. This pattern is highly reminiscent of the organization of the molecules in immature nodal complexes of normal animals (Poliak et al., 2001; Vabnick et al., 1999). It has been proposed that the developmental shift of $K^+$ channels and Caspr2 from paranodal to juxtaparanodal sites depends on the elaboration of transverse bands at the paranodes (Scherer and Arroyo, 2002). However, P0-deficient mice display an altered localization of juxtaparanodal molecules although they do form predominantly intact transverse axo-glial junctions as has been shown recently (Menichella et al., 2001). Thus, the presence of these structures appears not to be sufficient for a topologically correct distribution of $K^+$ channels and Caspr2. It has to be taken into further account that in P0-deficient mice, the dislocation of $K^+$ channels and Caspr2 is not as complete and uniform as seen in the galactocerebroside-, sulfatide- and PLP-mutants, but shows a more heterogeneous pattern with a high variability ranging from very few nodes with normal molecular organization of juxtaparanodes to nodal complexes completely devoid of Caspr2 and $K_v1.2$. The latter phenomenon might be at least partly brought about by the severe segmental de- and remyelination seen in P0−/− nerve fibers as has been described previously by conventional electron microscopy (Carenini et al., 1999; Giese et al., 1992; Martini et al., 1995a,b). Additionally, in P0−/− nerve fibers, $K_v1.2$ and Caspr2 often show an extension from their physiological juxtaparanodal compartment into the paranodal sites, rather than being completely shifted from juxtaparanodes to the paranodes. Similarly, a rather heterogeneous distribution for paranodal Caspr expression has also been observed in the P0-deficient mutants, particularly its asymmetrical presence at either side of the node. Again, this heterogeneous distribution of paranodal and juxtaparanodal proteins most probably reflects different stages of impaired myelination, demyelination and remyelination. In fact, demyelination and remyelination are also reflected here by some other features of immature nerve fibers, such as the shortening of internodal length and the presence of binary and broad VGSC clusters at the nodes of Ranvier. This is of particular interest since in Caspr-, contactin- and galactocerebroside-deficient mice, VGSCs and ankyrinG are clustered at the nodes (Bhat et al., 2001; Boyle et al., 2001; Dupree et al., 1999), though in a broader manner which is a feature reminiscent of an arrested development. It is, therefore, plausible to assume that nodal VGSC clustering per se does not depend on the cellular and molecular architecture of the paranodes (Bhat et al., 2001; Boyle et al., 2001; Dupree et al., 1999; Poliak et al., 2001), while the appearance of the VGSC clusters may be changed from the mature to broader forms upon paranodal alterations (Dupree et al., 1999; Ishibashi et al., 2002). This is consistent with previous findings that in normal PNS development, nodal VGSC clustering occurs before mature paranodal junction formation (Melendez-Vasquez et al., 2001).

The most striking finding in the mutants described here is that a lack of the compact myelin protein P0 leads to a change in the isoform determination of the VGSC at the node of Ranvier, namely, the upregulation of the TTX-resistant $Na_v1.8$. This is

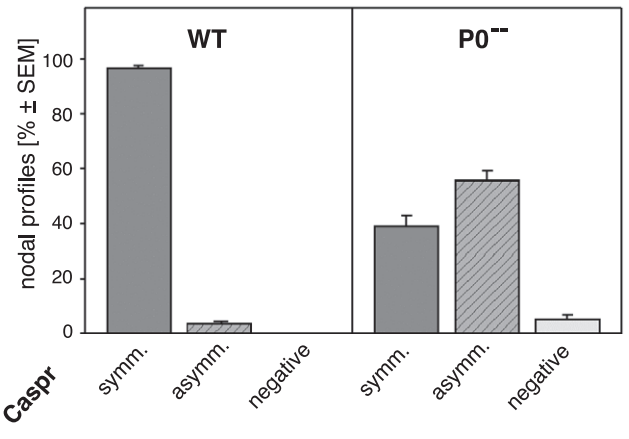


Fig. 4. In P0−/− nerve fibers, paranodal molecules are dislocated. In WT, Caspr is symmetrically localized at all paranodes, whereas P0−/− nodes are more often asymmetrically bordered by Caspr (hatched) or even sometimes devoid of paranodal Caspr. Nodal profiles in teased fiber preparations of femoral nerve quadriceps branch had been identified by either typical nodal $Na_v1.6$ or $Na_v1.8$ clusters and catagorized for the localization of paranodal Caspr staining.

particularly prominent in the motor nerves where this isoforrm is usually not expressed. Interestingly, Boiko et al. (2001) reported on an altered nodal VGSC isoform expression in CNS axons caused by a MBP mutation: In retinal ganglion cell (RGC) axons of shiverer mice, which are lacking compact myelin, the physiological nodal VGSC $Na_v1.6$ was markedly reduced and confined to the few remaining mature nodes, whereas $Na_v1.2$ was upregulated diffusely and predominantly present in hypomyelinated regions of RGC axons (Boiko et al., 2001). Additionally, in CNS of PLP transgenic mice (Rasband et al., 2003) and CNS as well as PNS of Caspr-deficient mice, $Na_v1.2$ is upregulated (Rios et al., 2003). This is in marked contrast to our findings in the peripheral nerve fibers of P0−/− mutants where $Na_v1.2$ expression could not be observed. In a recent study, Schwann cell-specific ablation of dystroglycan leads to myelin folding and downregulation of nodal $Na_v1.6$ expression. Similar to our observations, the $Na_v1.2$ isoform was not detectable in nodal regions (Saito et al., 2003). The expression of $Na_v1.8$ isoforms had not been investigated in these mutants.

The increase in $Na_v1.8$ expression in the dysmyelinating P0−/− mice seems to be in contrast to findings in the dysmyelinating *md* rat where the distribution of $Na_v1.8$-positive nodes was comparable to that of wild-type animals (Arroyo et al., 2002). However, in the hypomyelinating *taiep* rat, a mutant with progressive demyelination possibly due to an overexpression of oligodendrocytic microtubules, a substantial upregulation of $Na_v1.8$ in cerebellar Purkinje cells has been found (Black et al., 1999). Similarly, in chronic-relapsing experimental autoimmune encephalomyelitis (CR-EAE), an animal model related to multiple sclerosis (MS), $Na_v1.8$ was upregulated in cerebellar Purkinje cells as well (Black et al., 2000). Finally, autopsies from patients that suffered from a secondary progressive form of MS with cerebellar deficits showed a substantial upregulation of $Na_v1.8$ mRNA and protein in cerebellar Purkinje cells, whereas autopsies from control patients did not (Black et al., 2000). These findings suggest that the clinical phenotype of inherited and acquired CNS demyelination might not only be the result of defective electrical insulation and impaired propagation of axon potentials, but also the consequence of physiological abnormalities related to the ectopic expression of $Na_v1.8$. $Na_v1.8$ has been shown to mediate a robust and continuous firing pattern in response to sustained depolarization in DRG neurons and thus to contribute significantly to action potential electrogenesis in these cells (Renganathan et al., 2001). In particular, the aberrant coexpression of different types of VGSC, as it is seen in the P0−/− motor nerves described here, could lead to abnormal electrophysiological channel interactions. In addition to the overt consequences of impaired myelin formation like robustly impaired conduction properties (Zielasek et al.,1996), the abnormal channel interactions may produce spontaneous activity due to sub-threshold voltage oscillations supported by TTX-resistant VGSC and cross-activation of other VGSC (Waxman, 1999) as has been described for the sensory system (Rizzo et al., 1996). Taking these electrophysiological characteristics of $Na_v1.8$ as a TTX-resistant VGSC into account, it is possible that the neuromyotonic phenotype of P0-deficient mice (Vincent, 2000; Zielasek et al., 2000) is related to the characteristic bursting activity of the ectopically expressed $Na_v1.8$ channels and subsequent cross-activation of co-localized $Na_v1.6$ in P0−/− motor nerves. This question could be resolved by cross-breeding our P0-deficient mutants with knock-out mice deficient in the $Na_v1.8$ channel isotype (Akopian et al., 1999). Another factor that might impair the conduction properties of P0−/− fibers is the dislocation of $K^+$ channels. However, there are presently only poor data on the roles of these channels.

The ectopic expression of $Na_v1.8$ in the motor system of P0-deficient mice leads to the question of the possible mechanisms involved. For P0-deficient mutants, it is not yet known whether the upregulation of the $Na_v1.8$ channel is due to an increased mRNA transcription rate or due to a redistribution or an altered membrane targeting of pre-synthesized $Na_v1.8$ protein to the node of Ranvier that is normally degraded in mature motor neurons. Upregulation of $Na_v1.8$-specific mRNA as a response to pathological alterations within the CNS has been shown in the cerebellar Purkinje cells of the *taiep* rat (Black et al., 1999), of CR-EAE mice and of MS patients (Black et al., 2000). However, in the PNS, the regulation of $Na_v1.8$ as a response to nerve injury seems to be more complex. In an in vitro study, Hinson et al. (1997) could show upregulation of $Na_v1.8$ mRNA in cultured DRG neurons upon coculture with primary Schwann cells and upon addition of Schwann cell-conditioned medium. This is interesting because isolated Schwann cells dedifferentiate in a similar manner as denervated Schwann cells do upon Wallerian degeneration (Mirsky et al., 2002) and a comparable immature stage is displayed by Schwann cells of P0−/− mice (Giese et al., 1992). Similarly, a differential regulation of neuronal transcription of $Na_v1.8$ mRNA and axolemmal localization of $Na_v1.8$ protein has been described in DRG neurons under distinct pain conditions and in several lesion models (Black et al., 2002; Novakovic et al., 1998; Tanaka et al., 1998). Together with the findings obtained from our P0-deficient mice, a signalling cascade can be suggested which originates from the dysmyelinating Schwann cell, alters the molecular architecture and functional properties of axonal subdomains and probably affects the neuronal cell somata that may even be located within a healthy CNS environment. Such a signal cascade could finally lead to the well-described dysmyelination-induced axonal injury (Frei et al., 1999). Thus, myelin disorders may lead to altered expression patterns of axonal ion channels which confer at least partly the pathological features corresponding to an acquired channelopathy (Waxman, 2001a). Another mechanism might imply the consequences of infiltrating or activated immune cells, as has been speculated for $Na_v1.8$ upregulation in Purkinje cells of MS patients and in the corresponding animal models (Waxman, 2001b). In this context, it is worthwhile to mention that immune cells contribute to primarily genetically mediated demyelination in various kinds of myelin mutants (Carenini et al., 2001; Kobsar et al., 2003; Schmid et al., 2000) so that it is possible that humoral factors, such as cytokines and chemokines, might be involved in the dysregulation of the channel isotype. Since the myelin-related acquired channelopathies (Waxman, 2001a) might substantially contribute to the physiological consequences of impaired myelination and myelin maintenance, more research is necessary to characterize the mechanisms that regulate and dysregulate the localization of distinct isoforms of VGSCs in nodes of Ranvier.

## Experimental methods

### *Nerve fiber preparation and preparation of frozen sections*

Mice homozygously deficient for P0 were bred in our animal facility and their genotype was confirmed by routine PCR using

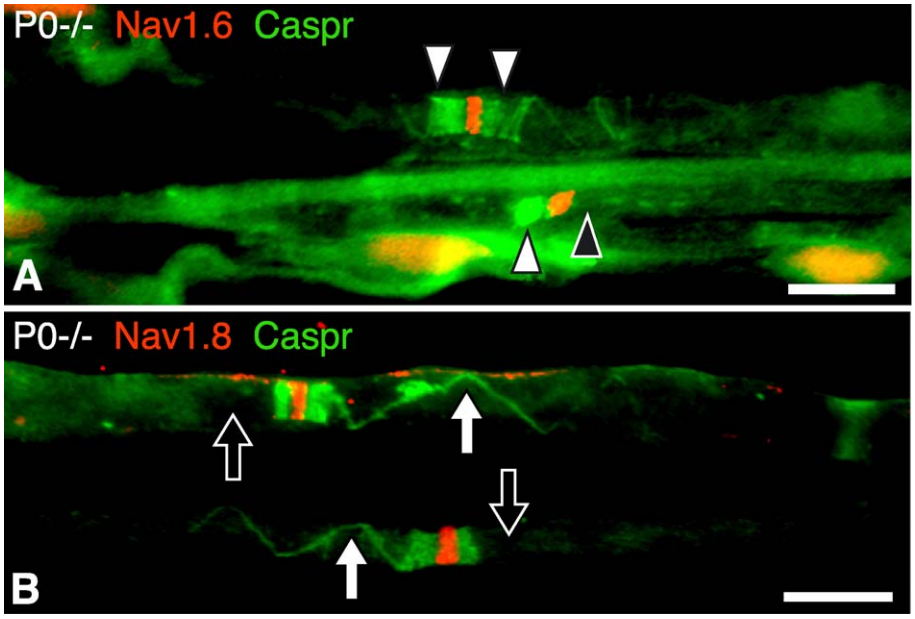
P0-/- Nav1.6 Caspr
A
P0-/- Nav1.8 Caspr
B

Fig. 5.

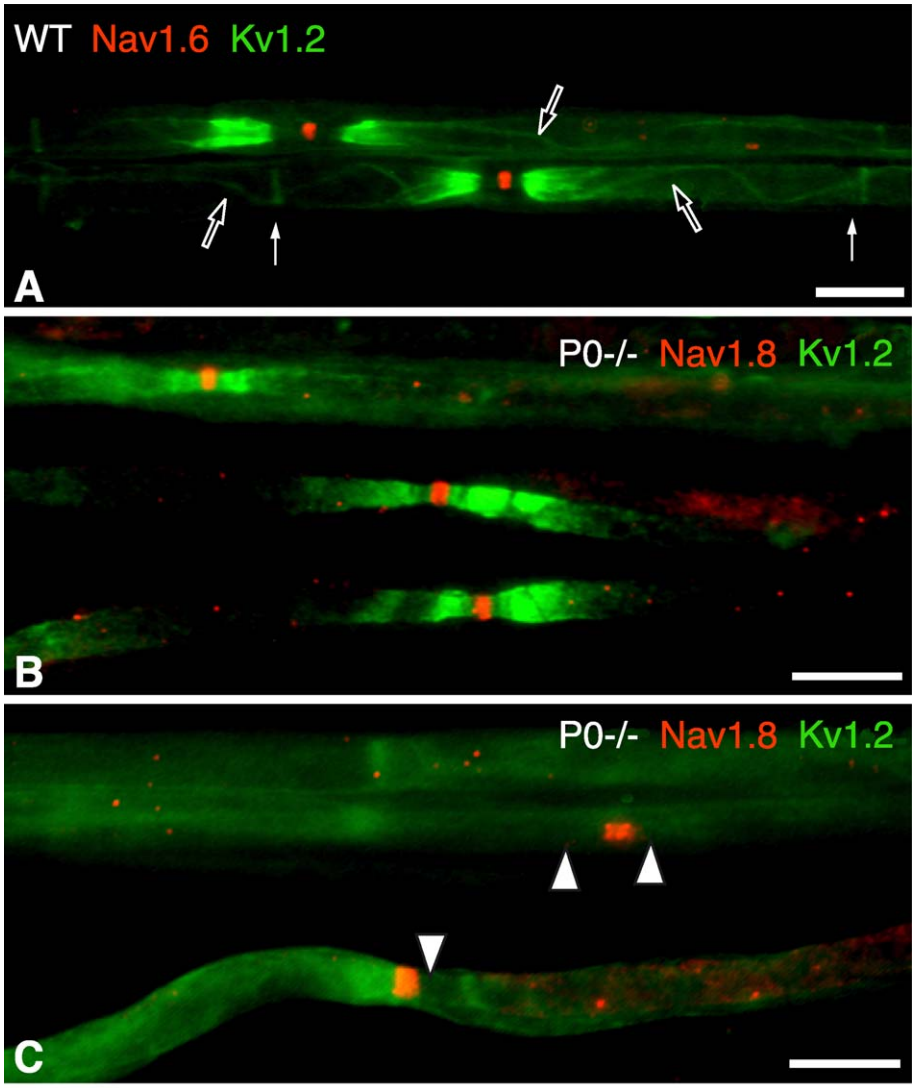
WT Nav1.6 Kv1.2
A
P0-/- Nav1.8 Kv1.2
B
P0-/- Nav1.8 Kv1.2
C

Fig. 6.

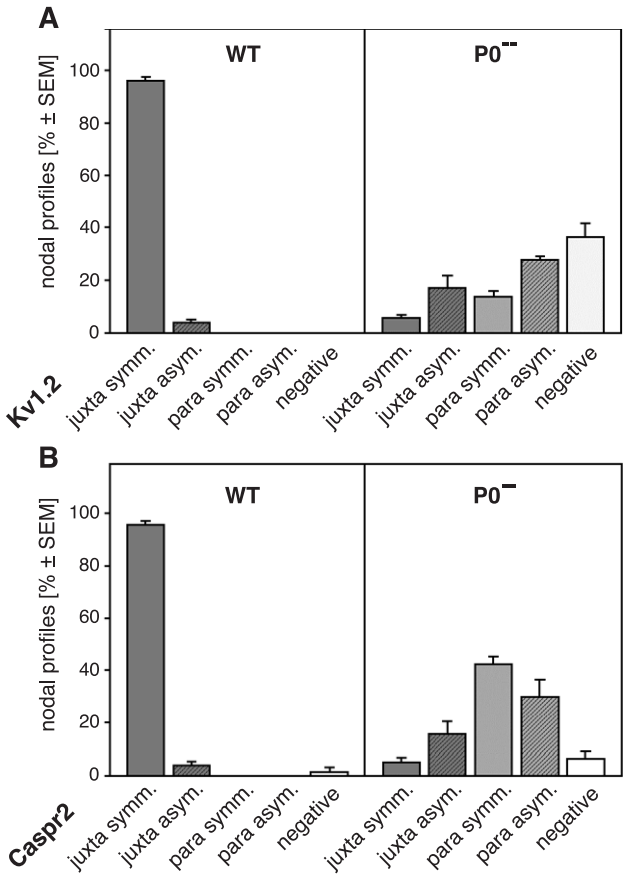


Fig. 7. In WT nerve fibers, $K_v1.2$ $K^+$ channels (A) and Caspr2 (B) are localized to the juxtaparanodes (“juxta”) symmetrically (“symm.”) flanking the nodes of Ranvier (first column). They are never paranodally (“para”) localized or absent (“negative”). P0 −/− fibers in contrast show a more variable and aberrant localization of $K_v1.2$ (A) and Caspr2 (B). Many nodal profiles display an extension of $K_v1.2$ and Caspr2 expression from the juxtaparanode to the paranode (“para”) or an asymmetry (“asym.”) with respect to juxtaparanodal or paranodal localization (hatched columns) and there is even a high percentage of nodal profiles entirely devoid of $K_v1.2$ (A, last column). Nodal profiles were identified by typical nodal immunofluorescence staining for $Na_v1.6$ or $Na_v1.8$ (A) or by paranodal immunofluorescence staining for Caspr (B), and categorized for the relative localization of $K_v1.2$ and Caspr2 immunofluorescence staining.

the specific primers as described previously (Schmid et al., 2000) and controlled for the typical phenotype characterized by early onset severe hindlimb paresis. P0−/− mice, 2.5 to 3 months old, and WT littermates were anesthetized by intraperitoneal injection of *S*-Ketamin (160 mg/kg; Pfizer, Karlsruhe) and Xylazine (16 mg/kg; Bayer, Leverkusen), thoracectomized and transcardially perfused for 10 min with phosphate-buffered saline (PBS) pH 7.4 containing 2% paraformaldehyde. Sciatic and femoral nerves were dissected and after removal, washed in PBS. Nerves were incubated in 0.5-fold PBS, manually unsheathed from epineurium and teased into single fibers using a pair of fine forceps on SuperFrost® Plus slides (Menzel, Germany). Slides were dried overnight at room temperature and then stored at −20 °C. Single fiber preparations of seven P0−/− mice and seven WT mice were pooled for further immunostaining studies. In addition, the sciatic and femoral nerves of two WT nerves were teased without prior fixation and used for immunostaining studies. As a positive control for antibodies against $Na_v1.2$, longitudinal fresh frozen sections of optic nerves of postnatal day 1 and 3-month-old WT mice (10 μm thick) were prepared and mounted on SuperFrost® Plus slides.

### *Immunocytochemistry*

Teased fiber preparations of perfused animals were postfixed in acetone at −20 °C for 10 min and washed in PBS. Teased fibers from non-perfused mice (see above) were not postfixed in acetone. Blocking and permeabilization was performed with PBS containing 0.3% Triton X-100, 4% normal goat serum (DAKO, Denmark) and 4% fetal calf serum (GIBCO, Germany) for 1 h (or 5% bovine serum albumin and 5% fetal calf serum for $Na_v1.2$ antibody). Primary antibodies were dissolved in blocking solution and incubated overnight at room temperature. Antibodies used were polyclonal affinity purified rabbit-anti-$Na_v1.6$ (AP848-5.2; Caldwell et al., 2000), rabbit-anti-$Na_v1.8$ (AP4154-4.2; Gould et al., 2000), goat-anti-$Na_v1.2$ (SC-16033; Santa Cruz, Heidelberg Germany) rabbit-anti-pan-$Na_v$ (AP1380-10.2; Dugandzija-Novakovic et al., 1995; Vabnick et al., 1996), rabbit-anti-pan-$Na_v$ (loops III and IV), monoclonal mouse-anti-$K_v1.2$ (both Upstate, Lake Placid, NY), rabbit-anti-$Na_v1.6$ (Scn8a), rabbit-anti-Caspr2 (both Chemicon, Temecula, CA), rabbit-anti-Caspr (intracellular domain; Peles et al., 1997) and mouse-anti-Caspr (extracellular domain; Poliak et al., 1999). After washing, fibers were incubated for 1 h at room temperature in Cy3-goat anti-rabbit-Ig and Cy2-goat anti-mouse-Ig (both Dianova, Hamburg). After mounting with coverslips and DABCO, epifluorescence microscopy was performed using a Zeiss Axiophot2 and digital images were acquired via a CCD-camera and ImagePro 4.0 software. Target specificity of the primary antibodies has been proved by preincubation of the antibodies used with an excess of the respective antigen peptide they were raised against (data not shown). For immunohistochemistry of fresh-frozen mouse optic nerve, sections were processed in exactly the same way as freshly teased nerve fibers as mentioned above.

Fig. 5. In P0−/− fibers, Caspr (green) is expressed at the paranode (A, white arrowheads), but often asymmetrically localized or absent (A, black arrowhead). In particular, its internodal expression along the inner mesaxon (B, white arrows) is frequently absent (B, black arrows) on one side of the node. The nodes are marked by $Na_v1.6$ or $Na_v1.8$, (red in A and B, respectively). Immunostained teased fiber preparation of mouse sciatic nerves. Scale bars, 10 μm.

Fig. 6. In WT nerve fibers (A), $K_v1.2$ potassium channels (green) are confined to the juxtaparanode and clearly separated form the node (marked by $Na_v1.6$, red). In the internodal axolemma, $K_v1.2$ is located along the opposing inner mesaxon (black arrows) and Schmidt–Lanterman incisures (white arrows). In P0 −/− nerve fibers (B–C), $K_v1.2$ (green) is frequently shifted from its juxtaparanodal sites to the paranode and very often no longer separated from the node (marked by $Na_v1.8$, red). Some nodes are even devoid of flanking $K^+$ channels (white arrowheads) at one or both sides of the node. Nodes are marked by immunoreactivity for $Na_v1.8$ (red in B and C). Teased fibers of femoral quadriceps (A and B) and sciatic nerve of 3 month-old WT (A) and P0 −/− mice (B and C). Scale bars, 10 μm.

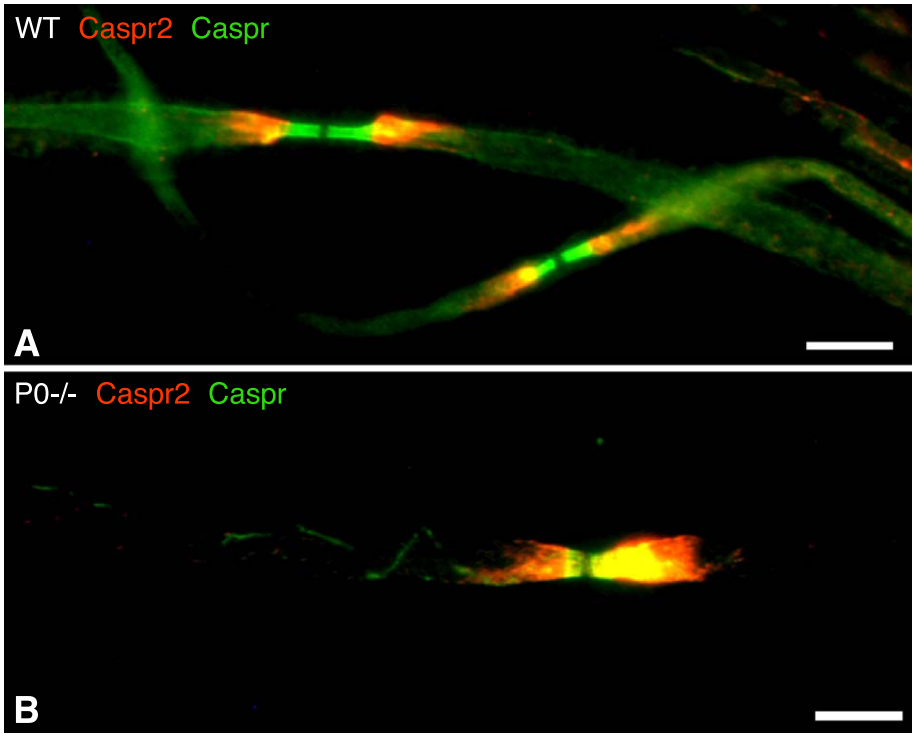


Fig. 8. In WT fibers (A), Caspr2 is localized to the juxtaparanode (red) and clearly separated from the paranode, marked by Caspr (green). By contrast, in P0−/− fibers (B), Caspr2 is often shifted to the paranode and there colocalized with Caspr (yellow merge). Teased fiber preparation of mouse sciatic nerves. Scale bars, 10 μm.

*Quantitative analysis*

Immunofluorescence-stained teased fiber preparations were analyzed for the number and morphology of nodal profiles in sciatic nerve, femoral quadriceps nerve and saphenous nerve separately. Nodal profiles were identified by paranodal flanking cuff-like Caspr staining or by typical nodal sodium channel clustering and then evaluated simultaneously for positivity or negativity of the respective ion channel isoforms. Single fibers were followed for their continuity and cumulative numbers of ion channel positive and negative nodal profiles were counted. These numbers were calculated as percentage of the total amount of counted nodal profiles (%) or expressed as density of channel clusters per fiber length counted [dimension ($mm^{-1}$)]. In the latter way, internodal length is another parameter that can additionally be accounted for. For each condition at least 60 mm (mean 159 mm for P0 − / −, mean 154 mm for WT), fiber length have been analyzed cumulatively. Data were collected in Excel™, analyzed with Systat 10™ and plotted with SigmaPlot 7.0™ software.

## Acknowledgments

The work was supported by the Deutsche Forschungsgemeinschaft, SFB581 (R.M.) and the Gemeinnützige Hertie-Stiftung (GHS 191/00/01; R.M.), and the National Multiple Sclerosis Society, Israel (E.P.). E.P. is an incumbent of the Madeleine Haas Russell Career Development Chair. C. Kiesel and H. Blazyca are given thanks for excellent technical assistance and H. Brünner for skillful animal care.

## References

Akopian, A.N., Sivilotti, L., Wood, J.N., 1996. A tetrodotoxin-resistant voltage-gated sodium channel expressed by sensory neurons. Nature 379, 257–262.

Akopian, A.N., Souslova, V., England, S., Okuse, K., Ogata, N., Ure, J., Smith, A., Kerr, B.J., McMahon, S.B., Boyce, S., Hill, R., Stanfa, L.C., Dickenson, A.H., Wood, J.N., 1999. The tetrodotoxin-resistant sodium channel SNS has a specialized function in pain pathways. Nat. Neurosci. 2, 541–548.

Arroyo, E.J., Scherer, S.S., 2000. On the molecular architecture of myelinated fibers. Histochem. Cell Biol. 113, 1–18.

Arroyo, E.J., Xu, T., Grinspan, J., Lambert, S., Levinson, S.R., Brophy, P.J., Peles, E., Scherer, S.S., 2002. Genetic dysmyelination alters the molecular architecture of the nodal region. J. Neurosci. 22, 1726–1737.

Baker, M.D., Wood, J.N., 2001. Involvement of Na+ channels in pain pathways. Trends Pharmacol. Sci. 22, 27–31.

Bennett, V., Lambert, S., 1999. Physiological roles of axonal ankyrins in survival of premyelinated axons and localization of voltage-gated sodium channels. J. Neurocytol. 28, 303–318.

Bhat, M., Rios, J., Lu, Y., Garcia-Fresco, G., Ching, W., St Martin, M., Li, J., Einheber, S., Chesler, M., Rosenbluth, J., Salzer, J.L., Bellen, H., 2001. Axon–glia interactions and the domain organization of myelinated axons requires neurexin IV/Caspr/Paranodin. Neuron 30, 369–383.

Black, J.A., Fjell, J., Dib-Hajj, S., Duncan, I.D., O'Connor, L.T., Fried, K., Gladwell, Z., Tate, S., Waxman, S.G., 1999. Abnormal expression of SNS/PN3 sodium channel in cerebellar Purkinje cells following loss of myelin in the *taiep* rat. NeuroReport 10, 913–918.

Black, J.A., Dib-Hajj, S., Baker, D., Newcombe, J., Cuzner, M.L., Waxman, S.G., 2000. Sensory neuron-specific sodium channel SNS is abnormally expressed in the brains of mice with experimental allergic encephalomyelitis and humans with multiple sclerosis. Proc. Natl. Acad. Sci. U. S. A. 97, 11598–11602.

Black, J.A., Dusart, I., Sotelo, C., Waxman, S.G., 2002. Axotomy does not up-regulate expression of sodium channel Nav1.8 in Purkinje cells. Mol. Brain Res. 101, 126–131.

Boiko, T., Rasband, M.N., Levinson, S.R., Caldwell, J.H., Mandel, G., Trimmer, J.S., Matthews, G., 2001. Compact myelin dictates the differential targeting of two sodium channel isoforms in the same axon. Neuron 30, 91–104.

Boyle, M.E., Berglund, E.O., Murai, K.K., Weber, L., Peles, E., Ranscht, B., 2001. Contactin orchestrates assembly of the septate-like junctions at the paranode in myelinated peripheral nerve. Neuron 30, 385–397.

Caldwell, J.H., Schaller, K.L., Lasher, R.S., Peles, E., Levinson, S.R., 2000. Sodium channel Nav1.6 is localized at nodes of Ranvier, dendrites, and synapses. Proc. Natl. Acad. Sci. U. S. A. 97, 5616–5620.

Carenini, S., Montag, D., Schachner, M., Martini, R., 1999. Subtle roles of neural cell adhesion molecule and myelin-associated glycoprotein during Schwann cell spiralling in P0-deficient mice. Glia 27, 203–212.

Carenini, S., Maurer, M., Werner, A., Blazyca, H., Toyka, K.V., Schmid, C.D., Raivich, G., Martini, R., 2001. The role of macrophages in demyelinating peripheral nervous system of mice heterozygously deficient in P0. J. Cell Biol. 152, 301–308.

Charles, P., Tait, S., Faivre-Sarrailh, C., Barbin, G., Gunn-Moore, F., Denisenko-Nehrbass, N., Guennoc, A.M., Girault, J.A., Brophy, P.J., Lubetzki, C., 2002. Neurofascin is a glial receptor for the Paranodin/Caspr-Contactin axonal complex at the axoglial junction. Curr. Biol. 12, 217–220.

Ching, W., Zanazzi, G., Levinson, S.R., Salzer, J.L., 1999. Clustering of neuronal sodium channels requires contact with myelinating Schwann cells. J. Neurocytol. 28, 295–301.

Coetzee, W., Amarillo, Y., Chiu, J., Chow, A., Lau, D., McCormack, T., Morena, H., Nadal, M., Ozaita, A., Pountney, D., Saganich, M., Vega-Saenz de Miera, E., Rudy, B., 1999. Molecular diversity of $K^+$ channels. Ann. N. Y. Acad. Sci. 868, 233–255.

Dugandzija-Novakovic, S., Koszowski, A.G., Levinson, S.R., Shrager, P., 1995. Clustering of Na+ channels and node of Ranvier formation in remyelinating axons. J. Neurosci. 15, 492–503.

Dupree, J.L., Girault, J.A., Popko, B., 1999. Axo-glial interactions regulate the localization of axonal paranodal proteins. J. Cell Biol. 147, 1145–1152.

Frei, R., Motzing, S., Kinkelin, I., Schachner, M., Koltzenburg, M., Martini, R., 1999. Loss of distal axons and sensory Merkel cells and features indicative of muscle denervation in hindlimbs of P0-deficient mice. J. Neurosci. 19, 6058–6067.

Giese, K., Martini, R., Lemke, G., Soriano, P., Schachner, M., 1992. Mouse P0 gene disruption leads to hypomyelination, abnormal expression of recognition molecules, and degeneration of myelin and axons. Cell 71, 565–576.

Girault, J.A., Peles, E., 2002. Development of nodes of Ranvier. Curr. Opin. Neurobiol. 12, 476–485.

Goldin, A.L., 1999. Diversity of mammalian voltage-gated sodium channels. Ann. N. Y. Acad. Sci. 868, 38–50.

Gould III, H.J., Gould, T.N., England, J.D., Paul, D., Liu, Z.P., Levinson, S.R., 2000. A possible role for nerve growth factor in the augmentation of sodium channels in models of chronic pain. Brain Res. 854, 19–29.

Hinson, A.W., Gu, X.Q., Dib-Hajj, S., Black, J.A., Waxman, S.G., 1997. Schwann cells modulate sodium channel expression in spinal sensory neurons in vitro. Glia 21, 339–349.

Ishibashi, T., Dupree, J.L., Ikenaka, K., Hirahara, Y., Honke, K., Peles, E., Popko, B., Suzuki, K., Nishino, H., Baba, H., 2002. A myelin galactolipid, sulfatide, is essential for maintenance of ion channels on myelinated axon but not essential for initial cluster formation. J. Neurosci. 22, 6507–6514.

Isom, L.L., 2001. Sodium channel beta subunits: anything but auxiliary. Neuroscientist 7, 42–54.

Jenkins, S.M., Bennett, V., 2001. Ankyrin-G coordinates assembly of the spectrin-based membrane skeleton, voltage-gated sodium channels, and L1 CAMs at Purkinje neuron initial segments. J. Cell Biol. 155, 739–746.

Jenkins, S.M., Bennett, V., 2002. Developing nodes of Ranvier are defined by ankyrin-G clustering and are independent of paranodal axoglial adhesion. Proc. Natl. Acad. Sci. U. S. A. 99, 2303–2308.

Kobsar, I., Berghoff, M., Samsam, M., Wessig, C., Mäurer, M., Toyka, K.V., Martini, R., 2003. Preserved myelin integrity and reduced axonopathy in connexin32-deficient mice lacking the recombination activating gene-1. Brain 126, 804–813.

Kordeli, E., Lambert, S., Bennett, V., 1995. AnkyrinG. A new ankyrin gene with neural-specific isoforms localized at the axonal initial segment and node of Ranvier. J. Biol. Chem. 270, 2352–2359.

Kozak, C.A., Sangameswaran, L., 1996. Genetic mapping of the peripheral sodium channel genes, Scn9a and Scn10a, in the mouse. Mamm. Genome 7, 787–788.

Krzemien, D.M., Schaller, K.L., Levinson, S.R., Caldwell, J.H., 2000. Immunolocalization of sodium channel isoform NaCh6 in the nervous system. J. Comp. Neurol. 420, 70–83.

Lambert, S., Davis, J.Q., Bennett, V., 1997. Morphogenesis of the node of Ranvier: co-clusters of ankyrin and ankyrin-binding integral proteins define early developmental intermediates. J. Neurosci. 17, 7025–7036.

Malhotra, J.D., Kazen-Gillespie, K., Hortsch, M., Isom, L.L., 2000. Sodium channel beta subunits mediate homophilic cell adhesion and recruit ankyrin to points of cell–cell contact. J. Biol. Chem. 275, 11383–11388.

Martini, R., Mohajeri, M.H., Kasper, S., Giese, K.P., Schachner, M., 1995a. Mice doubly deficient in the genes for P0 and myelin basic protein show that both proteins contribute to the formation of the major dense line in peripheral nerve myelin. J. Neurosci. 15, 4488–4495.

Martini, R., Zielasek, J., Toyka, K.V., Giese, K., Schachner, M., 1995b. Protein zero (P0)deficient mice show myelin degeneration in peripheral nerves characteristic of inherited human neuropathies. Nat. Genet. 11, 281–286.

Melendez-Vasquez, C.V., Rios, J.C., Zanazzi, G., Lambert, S., Bretscher, A., Salzer, J.L., 2001. Nodes of Ranvier form in association with ezrin-radixin-moesin (ERM)-positive Schwann cell processes. Proc. Natl. Acad. Sci. U. S. A. 98, 1235–1240.

Menichella, D.M., Awatramani, R., Xu, T., Baron, P., Vallat, J.M., Balsamo, J., Lilien, J., Scarlato, G., Kamholz, J., Scherer, S.S., Shy, M.E., 2001. Protein zero is necessary for E-cadherin-mediated adherens junction formation in Schwann cells. Mol. Cell. Neurosci. 18, 606–618.

Mirsky, R., Jessen, K.R., Brennan, A., Parkinson, D., Dong, Z., Meier, C., Parmantier, E., Lawson, D., 2002. Schwann cells as regulators of nerve development. J. Physiol. (Paris) 96, 17–24.

Novakovic, S.D., Tzoumaka, E., McGivern, J.G., Haraguchi, M., Sangameswaran, L., Gogas, K.R., Eglen, R.M., Hunter, J.C., 1998. Distribution of the tetrodotoxin-resistant sodium channel PN3 in rat sensory neurons in normal and neuropathic conditions. J. Neurosci. 18, 2174–2187.

Novakovic, S.D., Eglen, R.M., Hunter, J.C., 2001. Regulation of Na+ channel distribution in the nervous system. Trends Neurosci. 24, 473–478.

Peles, E., Salzer, J.L., 2000. Molecular domains of myelinated axons. Curr. Opin. Neurobiol. 10, 558–565.

Peles, E., Nativ, M., Lustig, M., Grumet, M., Schilling, J., Martinez, R., Plowman, G.D., Schlessinger, J., 1997. Identification of a novel contactin-associated transmembrane receptor with multiple domains implicated in protein–protein interaction. EMBO J. 16, 978–988.

Poliak, S., Gollan, L., Martinez, R., Custer, A., Einheber, S., Salzer, J.L., Trimmer, J.S., Shrager, P., Peles, E., 1999. Caspr2, a new member of the neurexin superfamily, is localized at the juxtaparanodes of myelinated axons and associates with K+ channels. Neuron 24, 1037–1047.

Poliak, S., Gollan, L., Salomon, D., Berglund, E.O., Ohara, R., Ranscht, B., Peles, E., 2001. Localization of Caspr2 in myelinated nerves depends on axon–glia interactions and the generation of barriers along the axon. J. Neurosci. 21, 7568–7575.

Rasband, M.N., Trimmer, J.S., 2001. Developmental clustering of ion channels at and near the node of Ranvier. Dev. Biol. 236, 5–16.

Rasband, M.N., Peles, E., Trimmer, J.S., Levinson, S.R., Lux, S.E., Shrager, P., 1999. Dependence of nodal sodium channel clustering

on paranodal axoglial contact in the developing CNS. J. Neurosci. 19, 7516–7528.

Rasband, M.N., Kagawa, T., Park, E.W., Ikenaka, K., Trimmer, J.S., 2003. Dysregulation of axonal sodium channel isoforms after adult-onset chronic demyelination. J. Neurosci. Res. 73, 465–470.

Renganathan, M., Cummins, T.R., Waxman, S.G., 2001. Contribution of Nav1.8 sodium channels to action potential electrogenesis in DRG neurons. J. Neurophysiol. 86, 629–640.

Rios, K.C., Rubin, M., St. Martin, M., Downey, R.T., Einheber, S., Rosenbluth, J., Levinson, S.R., Bhat, M., Salzer, J.L., 2003. Paranodal interactions regulate expression of sodium channel subtypes and provide a diffusion barrier for the node of Ranvier. J. Neurosci. 23, 7001–7011.

Rizzo, M.A., Kocsis, J.D., Waxman, S.G., 1996. Mechanisms of paresthesiae, dysesthesiae and hyperesthesiae: role of Na+ channel heterogeneity. Eur. Neurol. 36, 3–12.

Saito, F., Moore, S.A., Barresi, R., Henry, M.D., Messing, A., Ross-Barta, S., Cohn, R.D., Willamson, R.A., Sluka, K.A., Sherman, D.L., Brophy, P.J., Schmelzer, J.D., Low, P.A., Wrabetz, L., Feltri, M.L., Campbell, K.P., 2003. Unique role of dystroglycan in peripheral nerve myelination, nodal structure, and sodium channel stabilization. Neuron 38, 747–758.

Sangameswaran, L., Delgado, S.G., Fish, L.M., Koch, B.D., Jakeman, L.B., Stewart, G.R., Sze, P., Hunter, J.C., Eglen, R.M., Herman, R.C., 1996. Structure and function of a novel voltage-gated, tetrodotoxin-resistant sodium channel specific to sensory neurons. J. Biol. Chem. 271, 5953–5956.

Scherer, S.S., Arroyo, E.J., 2002. Recent progress on the molecular organization of myelinated axons. J. Peripher. Nerv. Syst. 7, 1–12.

Schmid, C.D., Stienekemeier, M., Oehen, S., Bootz, F., Zielasek, J., Gold, R., Toyka, K.V., Schachner, M., Martini, R., 2000. Immune deficiency in mouse models for inherited peripheral neuropathies leads to improved myelin maintenance. J. Neurosci. 20, 729–735.

Tanaka, M., Cummins, T.R., Ishikawa, K., Dib-Hajj, S.D., Black, J.A., Waxman, S.G., 1998. SNS Na+ channel expression increases in dorsal root ganglion neurons in the carrageenan inflammatory pain model. NeuroReport 9, 967–972.

Traka, M., Dupree, J.L., Popko, B., Karagogeos, D., 2002. The neuronal adhesion protein TAG-1 is expressed by Schwann cells and oligodendrocytes and is localized to the juxtaparanodal region of myelinated fibers. J. Neurosci. 22, 3016–3024.

Tzoumaka, E., Tischler, A.C., Sangameswaran, L., Eglen, R.M., Hunter, J.C., Novakovic, S.D., 2000. Differential distribution of the tetrodotoxin-sensitive rPN4/NaCh6/Scn8a sodium channel in the nervous system. J. Neurosci. Res. 60, 37–44.

Vabnick, I., Novakovic, S.D., Levinson, S.R., Schachner, M., Shrager, P., 1996. The clustering of axonal sodium channels during development of the peripheral nervous system. J. Neurosci. 16, 4914–4922.

Vabnick, I., Trimmer, J.S., Schwarz, T.L., Levinson, S.R., Risal, D., Shrager, P., 1999. Dynamic potassium channel distributions during axonal development prevent aberrant firing patterns. J. Neurosci. 19, 747–758.

Vincent, A., 2000. Understanding neuromyotonia. Muscle Nerve 23, 655–657.

Waxman, S.G., 1999. The molecular pathophysiology of pain: abnormal expression of sodium channel genes and its contributions to hyperexcitability of primary sensory neurons. Pain 82, S133–S140.

Waxman, S.G., 2001a. Acquired channelopathies in nerve injury and MS. Neurology 56, 1621–1627.

Waxman, S.G., 2001b. Transcriptional channelopathies: an emerging class of disorders. Nat. Rev. Neurosci. 2, 652–659.

Zielasek, J., Martini, R., Toyka, K.V., 1996. Functional abnormalities in P0-deficient mice resemble human hereditary neuropathies linked to P0 gene mutations. Muscle Nerve 19, 946–952.

Zielasek, J., Martini, R., Suter, U., Toyka, K.V., 2000. Neuromyotonia in mice with hereditary myelinopathies. Muscle Nerve 23, 696–701.